Journal of Applied Polymer Science

Characteristics and 3D Formation of PVA and PEO Electrospun Nanofibers with Embedded Urea

Ibrahim Hassounah,[1] Nader Shehata,[2,3] Amanda Hudson,[4] Bruce Orler,[1,4] Kathleen Meehan[2]

[1]Institute for Critical Technology and Applied Sciences (ICTAS), Virginia Polytechnic Institute and State University, Blacksburg, Virginia 24061

[2]The Bradley Department of Electrical and Computer Engineering (ECE), Virginia Polytechnic Institute and State University, Blacksburg, Virginia 24061

[3]Department of Engineering Mathematics and Physics, Faculty of Engineering, Alexandria University, Alexandria 21526, Egypt

[4]Department of Chemistry, Virginia Polytechnic Institute and State University, Blacksburg, Virginia 24061

Correspondence to: I. Hassounah (E-mail: Ibrahim.Hassounah@gmail.com)

ABSTRACT: The behavior of electrospun polyvinyl alcohol (PVA) and polyethylene oxide (PEO) nanofibers embedded with urea is studied as a function of various process parameters. Our results show that three-dimensional nanofiber networks can be obtained when high concentrations of urea in the solution are used during electrospinning. The nanofibers are characterized using both scanning electron microscope (SEM) and Fourier transform infrared spectroscopy (FTIR). The stability of the nanofiber as a function of electric field has also been studied. The successful formation of three-dimensional nanofiber networks can open new trends toward applications in fertilizers containing nanofibers in the nanoagricultural field. © 2013 Wiley Periodicals, Inc. J. Appl. Polym. Sci. **2014**, *131*, 39840.

KEYWORDS: electrospinning; nanostructured polymers; biodegradable; urea fibers

Received 2 April 2013; accepted 8 August 2013

DOI: 10.1002/app.39840

INTRODUCTION

Among the different natural and chemical fertilizers used for plant cultivation, urea has been found to be one of the best choices as a nitrogen release fertilizer.[1] Urea has the highest nitrogen content per unit mass or volume (46% of its mass nitrogen content) and has the lowest transport costs.[2,3] Although urea has many advantages, it is considered to be harmful for farmers through skin exposure or inhalation.[4] For example, urea can cause irritation to the skin or respiratory tracts through inhalation, especially at high concentrations.[5] Therefore, there is a strong demand to protect farmers during fertilization in the cultivating process. Encapsulation of urea granules is employed to control the release of urea to the soil; however, it is also a helpful tool to protect farmers from skin irritation by direct contact.[6] Urea embedded in nanofibers can be another possible mean to distribute the fertilizing compound with reduced risk to farmers as there will be minimal direct contact with skin or inhalation of urea dust.

Electrospinning is selected as the fabrication method for the urea-embedded nanofibers because the simplicity of operation, the feasibility to embed compounds such as urea in the resulting nanofibers, and the potential for scale-up to manufacture large volumes.[7] Electrospinning is a process in which electrostatic field across the tip of a needle and a metallic target causes charged polymeric material to flow from the tip towards the target, producing a nanofiber.[8–10] As the polymer jet flies toward the target, it undergoes stretching and thinning processes through different kinds of instabilities: electric field-induced instability, varicose instability, and whipping or bending instability,[11–13] as shown in Figure 1. These instabilities are due to the repulsion of charges on the jet surface.[14,15]

Electric field-induced instability arises from homogeneous axial repulsions of charges on the jet's surface.[16,17] It corresponds to the straight jet before bending occurs, and it could be combined with small lateral fluctuation in the centerline of the polymer jet.[18] Varicose instability appears when the straight jet centerline starts to vibrate and immediately before the bending instability starts to be occurred.[19] In the inverted conical envelope region of the jet, bending or whipping instability is developed by non-symmetric charge repulsions.[20] It occurs at some distance away from the droplet tip.[13,19] Bending instability can be reduced at high electric field strengths and high flow rates, resulting in the formation of straight jets along the distance between electrodes.[19]

Many attempts have been made to fabricate nanofibers containing high amount of urea, but the process have been shown

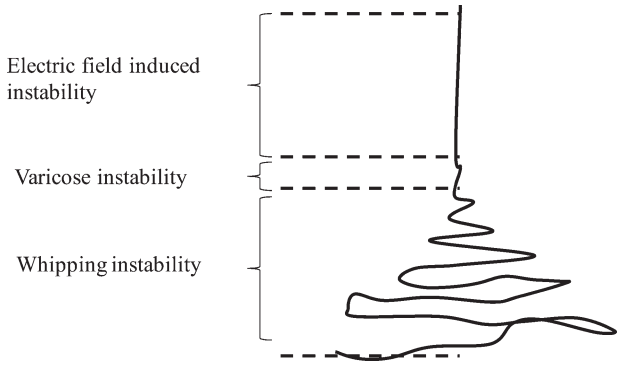

Figure 1. Schematic diagram of electrospinning jet shows the different regions of instabilities.

problematic. Liu et al. in 2008 and Isakov et al. in 2010 electrospun PEO and PVA nanofibers containing urea.[21,22] Both research groups studied the optical characteristics of the urea embedded nanofibers. In addition, the fibers were further characterized by Liu et al. using wide angle X-ray diffraction (WAXD) and differential scanning calorimetry (DSC). PEO nanofibers with embeded urea up to 15% were produced by Celebioglu et al., but the authors reported the difficulty of producing fibers containing urea above 15% as the fibers are converted into debris.[23] Shinji et al. investigated three different techniques to create nanofibers containing urea crystallites: mix-spin, Langmuir–Blodgett-spin, and Langmuir–Blodgett-natural drying methods, using an array of core-shell particles as the template.[24] Although Shinji et al. obtained nanofibers that incorporated large concentrations of urea (up to 40%), the techniques studied to create these urea-embedded nanofibers are not suitable to scaled up for industrial mass production.

PVA and PEO are well known as non-toxic biodegradable water soluble polymers.[25,26] This characteristic is critical for many applications such as nanoagriculture, tissue engineering, and other biomedical applications.[27–31] The slow biodegradation rate of PEO compared to PVA and PVA/PEO blends makes it the preferable polymer to utilize in applications where the release rate of active materials, such as drugs and fertilizers, embedded in the nanofibers must be controlled for long time periods, with some studies demonstrating that the nanofibers can remain for up to 34 days.[32–35] Thus, PEO is the most attractive of the three polymers when electrospinning nanofibers that containing urea for nanoagriculture applications where the fertilizer must be released slowly over a month while either urea-embedded nanofibers composted of PVA or a PVA/PEO blend are good candidates when a rapid release of the fertilizer is required.

In this article, the properties of PVA, PVA/PEO, and PEO nanofibers with embedded urea are evaluated as a function of the chemical composition of the fiber precursors and the processing parameters. The physical properties of the nanofibers, fiber diameters and morphology, are measured from images obtained using a scanning electron microscope (SEM). Also, the optimum process conditions to form three-dimensional (3D) electrospun nanofibers embedded with urea have been identified. The porosity of 3D mats formed of nanofibers can be higher than mats consist of microfibers. This feature can enable a large volume of water to be captured within the voids of the 3D mat, which may be advantageous as it may allow farmers to reduce the amount of water required for irrigation because water can be introduced into the soil along with the urea-embedded nanofibers and the 3D mat can slowly release moisture trapped in the mat during rainstorms or during irrigation. Fourier transform infrared spectroscopy (ATR-FTIR) is used to study the interaction between urea and the polymers, which is important to determine the viability of the embedded urea as a fertilizer. Finally, the influence of the electric field intensity and electrode polarity on the development of instabilities during the formation of the nanofibers is discussed.

EXPERIMENTAL WORK

Materials

PVA (Dupont, Taipei, Taiwan) with degree of hydrolysis of 88%, PEO of molecular weight 300,000 g/mol, and urea (both from Sigma-Aldrich, St. Louis, MO) are the materials used to form the electrospun fibers. PVA and PEO are dissolved in deionized water at concentrations 13 and 8 wt %, respectively. These concentrations are chosen as the authors had found this to be the optimal concentration to produce electrospun mats with minimal visual defects such as pinholes or wet fleeces. Once the PVA and PEO are dissolved in water, urea is added to the polymer solution and the mixture is stirred for 24 h before the electrospinning process is initiated. The maximum

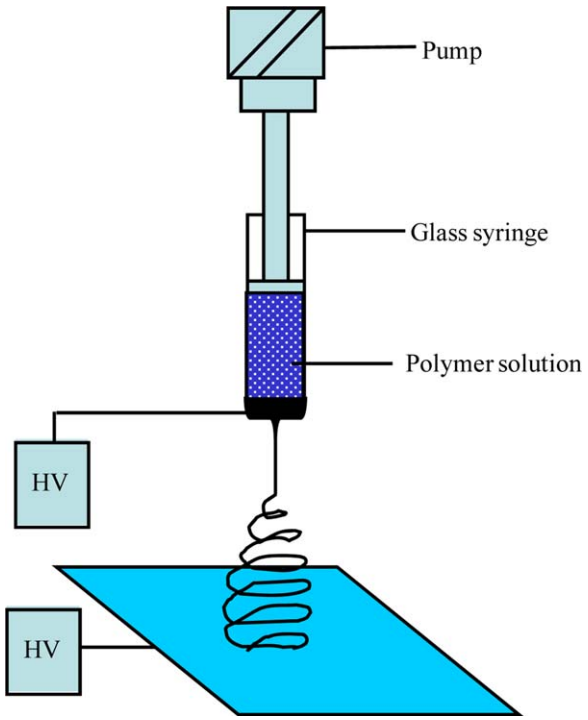

Figure 2. Schematic illustration of the setup of the electrospinning device. [Color figure can be viewed in the online issue, which is available at wileyonlinelibrary.com.]

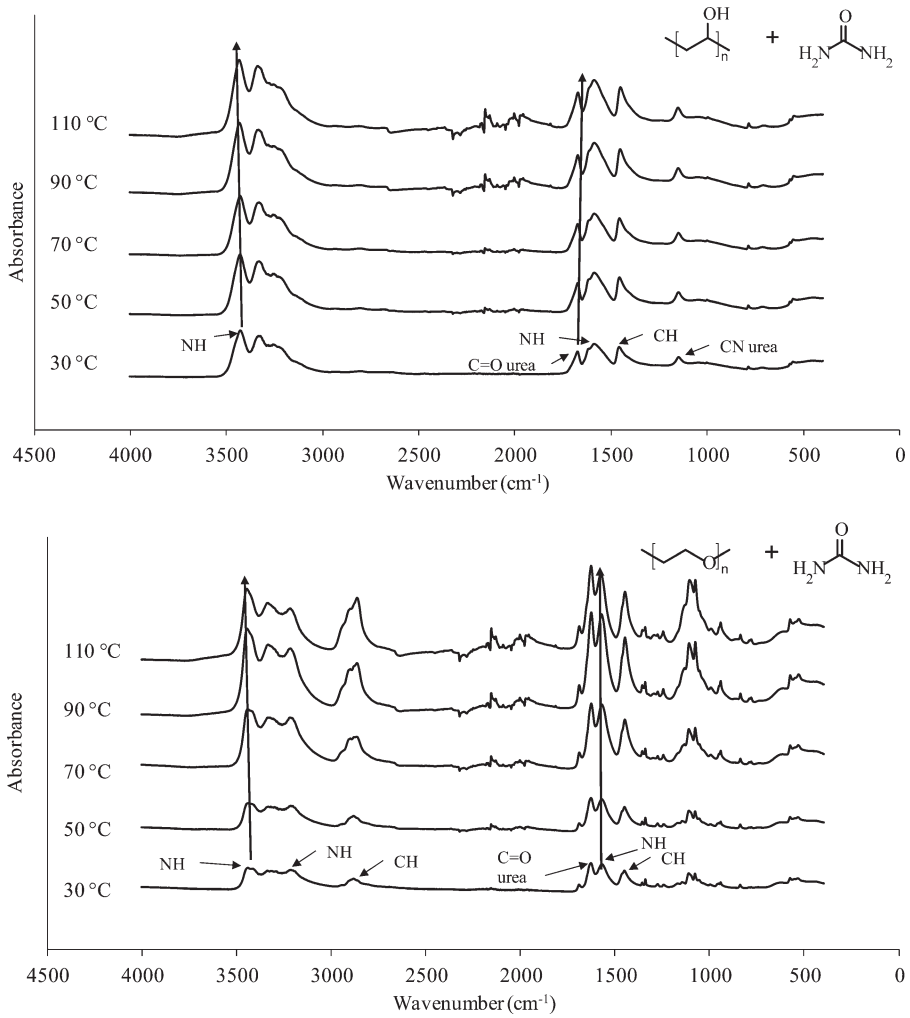

Figure 3. FESEM images of: A: PVA nanofibers fabricated from solutions with no urea, B: PVA nanofibers electrospun from solutions containing 20 wt % urea, C: PEO nanofibers with fabricated from solutions with no urea, and D: PEO nanofibers electrospun from solutions containing 20 wt % urea.

concentration of urea used in this study is 25% of the total weight of polymer solutions.

Electrospinning

The electrospinning setup, as shown in Figure 2, consists of a 10 mL plastic syringe with 18 gauge metallic needle that will be the source of the charged droplets that form the polymer jet, a single polarity, variable high voltage (0–15 kV) power supply (Gamma High Voltage Research, Inc. model ES40) that is connected to the needle of the syringe, an adjustable high voltage power supply (0–30 kV) with two different polarities (Spellman High Voltage Electronics Corporation model CZE1000R) that is connected to the aluminum foil-covered target, and a syringe pump (New Era Pump, Inc. model NE-300). The distance between the needle tip and the target is held constant at 15 cm. The difference in voltage between the needle and target is varied over the range from 15 kV to 25 kV. The flow rate of the polymer solution supplied to the syringe is fixed at 1 mL/h. The polarities of the two voltage generators are used to guide the polymer jet aroused from the needle directly towards the target. The samples are collected on a flat metallic surface covered with aluminum foil. Each deposition of electrospun fibers is run for a total of 30 min with the result that a nonwoven fiber web coats the target. During the experiments in which the polarity of the electric field between the needle and target is switched, high voltage supply that is connected to the aluminum foil target is switched off and the target is used as a grounded electrode while the high voltage supply connected to the syringe remains on.

Characterization

The dimensions of the electrospun fibers are characterized using a Zeiss LEO 1550 field emission scanning electron microscopy (FESEM) to determine the morphology of the fiber web and the diameter and homogeneity of the individual fibers. The fiber diameters are measured by Image-J software and the webs are imaged by a digital camera (Canon EOS 60D CMOS sensor). Another characterization method is performed with FTIR spectroscopy (Varian 670-IR with PIKE GladiATR accessory) over a temperature range from 30°C to 110°C to detect the existence of hydrogen bonding formed between urea and the polymers through the absorption of carbonyl, amino, and hydroxyl groups.

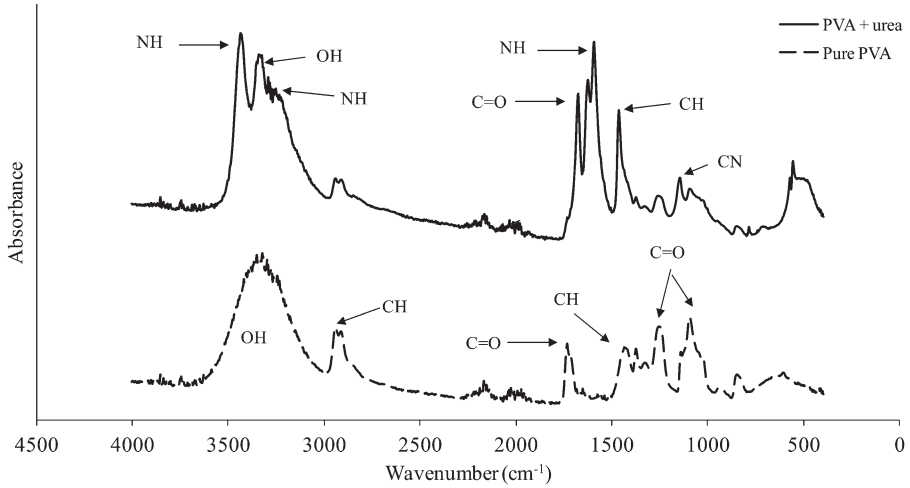

Figure 4. FTIR spectra collected from (A) PVA and (B) PEO nanofibers both containing urea, where the measured temperature are increased from 30°C to 110°C with increments of 20°C step. Characteristic absorption lines for N—H, C—H, and the C═O and C—N bonds in urea are labeled. The shown chemical formulas are related to PVA with urea and PEO with urea in Figures A and B, respectively.

RESULTS AND DISCUSSION

Characterization of Electrospun Fibers

Representative images of PVA nanofibers without and with 20% urea are shown in Figure 3(A,B) and images of PEO nanofibers without and with 20% urea are shown in Figure 3(C,D). It is clear that electrospinning from PVA solutions containing 20 wt % urea produce fused fibers whereas individual nanofibers are formed from PVA solutions that do not contain urea. The morphology of PEO nanofibers containing urea is unchanged from that obtained when the PEO nanofibers do not contain urea. It is speculated that the fused PVA nanofibers could be due to the incomplete evaporation of water from the polymer jet before solidification on the target. The diameters of the PVA and PEO nanofiber range from 200 to 400 nm in Figure 3(A,C,D).

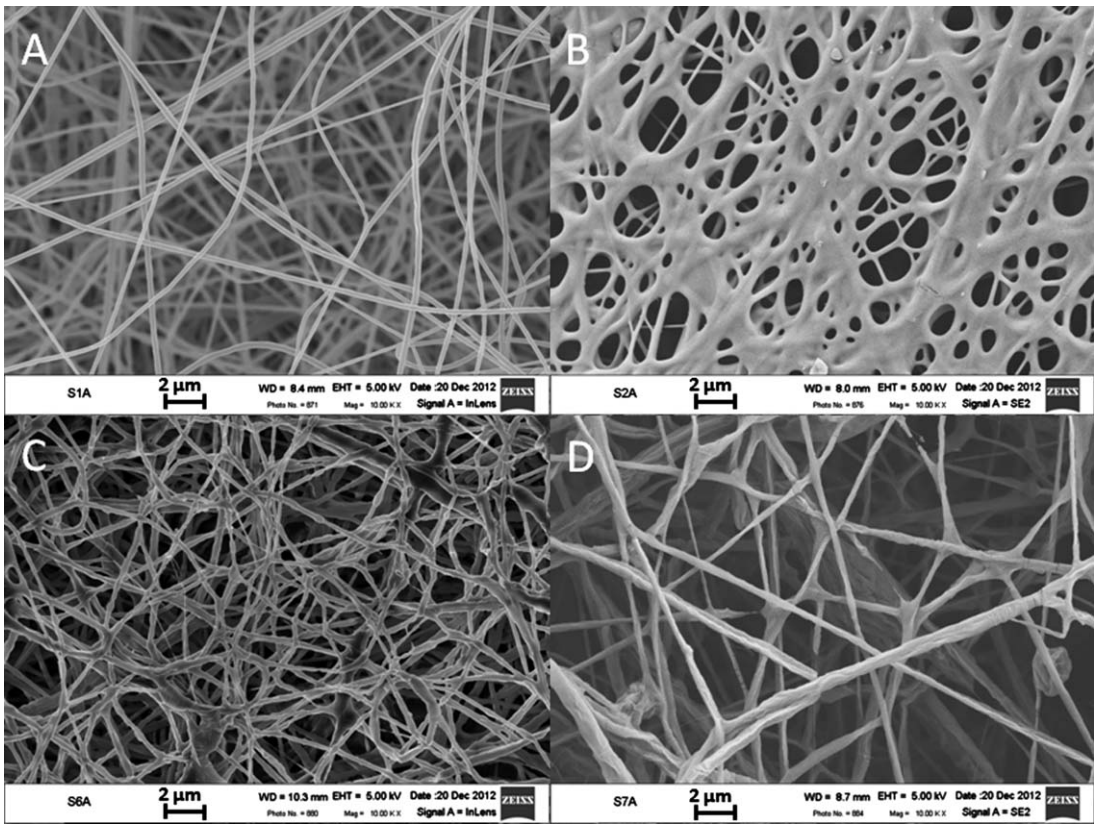

Figure 5. FTIR spectra for pure PVA nanofibers and PVA nanofibers containing urea showing the reduction of the CH peak between 2800 and 3000 cm^{-1} upon addition of urea.

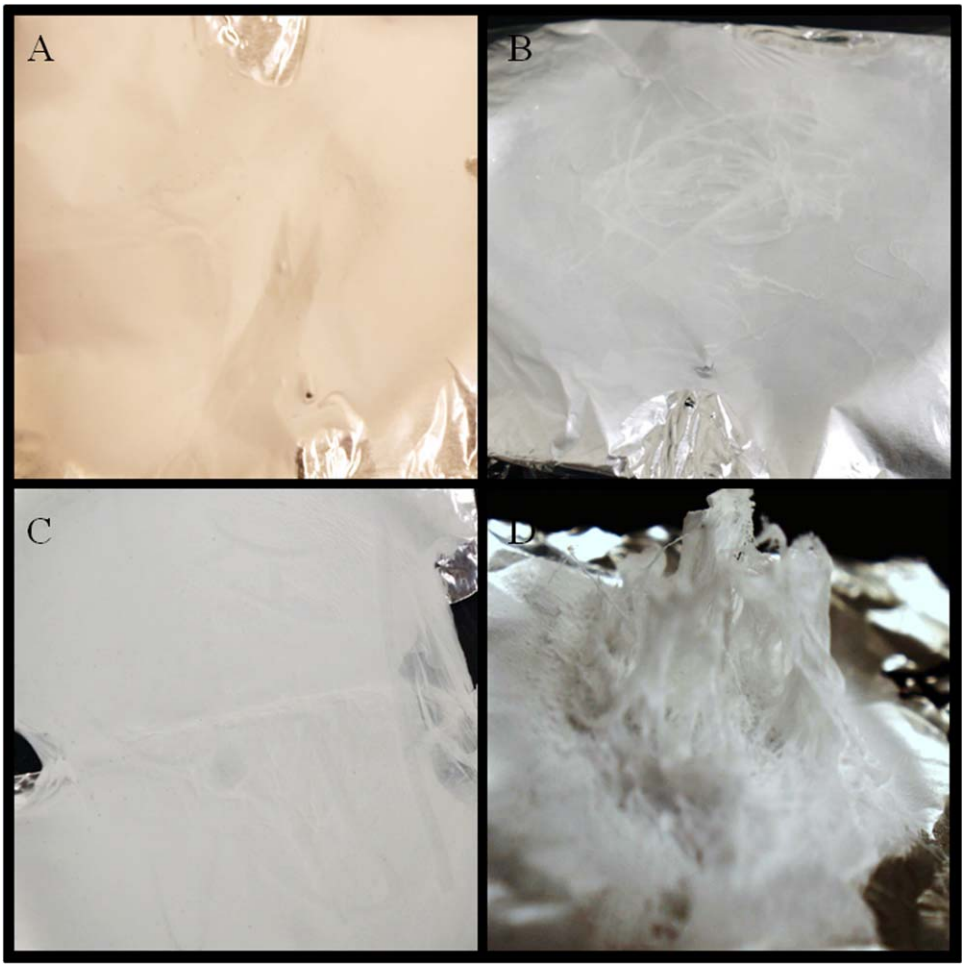

Figure 6. Images of electrospun nanofibers with embedded urea prepared using (A) PVA with no urea, (B) PVA with 20 wt % urea, (C) PEO with no urea, and (D) PEO with 20 wt % urea. [Color figure can be viewed in the online issue, which is available at wileyonlinelibrary.com.]

However, the diameter of the fused nanofibers in Figure 3(B) varies from 150 to 430 nm.

FTIR spectra analysis in Figure 4 shows that hydrogen bonds, H-bonds, are formed between urea (through its amino and carbonyl groups) and the polymers (through their ether and hydroxyl groups). As the temperature of the nanofibers is increased, the peaks intensities are generally increased and there is a cleavage of the H-bonds. This is shown in Figure 4 where the small shift of both amino and carbonyl peaks, located in IR region, to higher wavelengths indicates the cleavage of the H-bonds. The hydrogen bonds between PEO and urea are more easily broken than the hydrogen bonds between PVA and urea because the polarity of ether bonds (C—O—C) in PEO is less than the polarity of alcohol bonds (C—OH) in PVA. This difference in polarity means that there are relatively weaker hydrogen bonds between urea and PEO

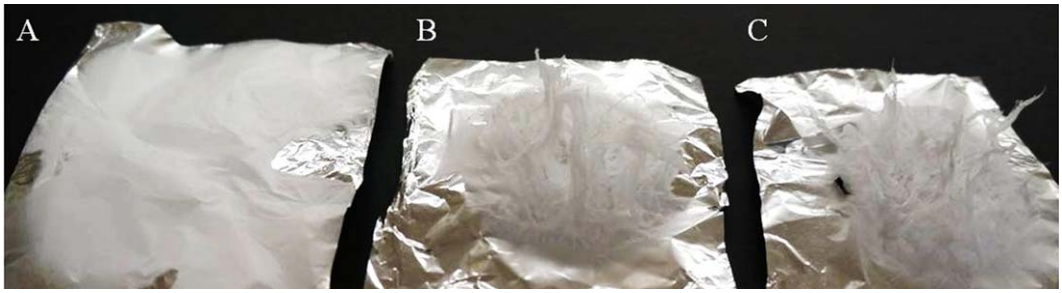

Figure 7. Images of electrospun PEO nanofibers with (A) 0 wt % embedded urea, (B) 20 wt % urea, and (C) 25 wt % urea that demonstrate that there is an increase in the thickness of the three-dimensional web of fibers as the urea content of the polymeric solution is increased. [Color figure can be viewed in the online issue, which is available at wileyonlinelibrary.com.]

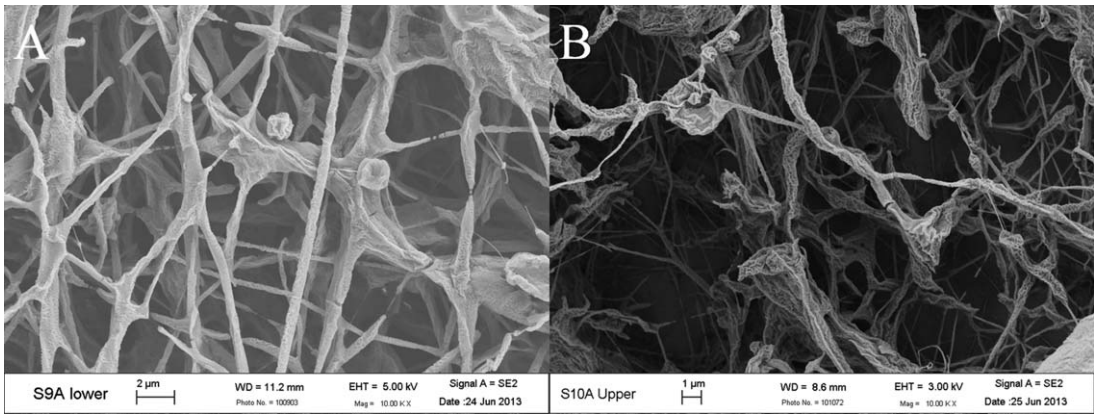

Figure 8. SEM images of the 3D electrospun PEO nanofibers with (A) 20 wt % embedded urea and (B) 25 wt % urea.

than between urea and PVA.[36] Therefore, more energy is required to break the hydrogen bonds in the PVA matrix than to break the bonds in the PEO matrix. This result is significant because it demonstrates that a portion of urea incorporated in the nanofibers will not be released easily from either polymer matrix at room temperature and that the urea is more tightly bound within the PVA nanofibers. Urea can liberate easily from the PEO polymer chains rather than in case of PVA polymer chains, which means that PEO is likely a better choice for a timed release of urea for use as fertilizer. Even though the polymer mats can dissolve in water, some of the urea will remain bound to the polymer molecules, especially to PVA, and, thus, not all of the urea embedded in the nanofibers will be available as fertilizer. Additionally, as PVA is consumed by soil microorganisms faster than PEO, the strongly attached urea to the PVA can be consumed as well.[37]

The consumed urea will also be hydrolyzed by the microorganisms into carbon dioxide and ammonia which can be toxic to plants above certain concentrations.[4] The questions as to how much urea embedded in the PVA would be converted to ammonia and whether the result is at a sufficient concentration to harm crop plants will be investigated further. On the basis of an evaluation of the research conducted thus far, it is concluded that PEO electrosupun nanofibers is a better choice for the polymer matrix to deliver urea to crop plants rather than PVA nanofibers. As ATR-FTIR is surface analyzing technique,[38] we speculate that urea is distributed homogenously on the surface of nanofibers, bounded by H-bond with alcholoic or ester oxygen. This is why the characterizing peak for CH at 2800–3000 cm^{-1} becomes much reduced as shown in Figure 5.

Impact of Urea Concentration

PEO and PVA solutions containing different amounts of urea are used to electrospun nanofibers at electric field strength of 1 kV/cm, where a positive voltage has been applied to the needle and a negative voltage is applied to the target. Three-dimensional webs of nanofibers are observed when the solution electrospun is PEO containing at least 20 wt %, urea while the morphology of the electrospun PVA nanofibers with 20 wt % urea are flat, as shown in Figure 6. Here, 3D webs means that nanofibers are deposited randomly in three dimension structure with an observable height. The thickness of the three-dimensional fibers within PEO mats increases from 760 μm to 2 cm as the concentration of urea in the polymer solution is altered from 0 to 25 wt % (Figure 7). SEM images of the formed 3D nanofibers at different urea concentration are shown in Figure 8. Generally the fiber diameters did not vary significantly by increasing the concentration of urea, i.e., the fiber

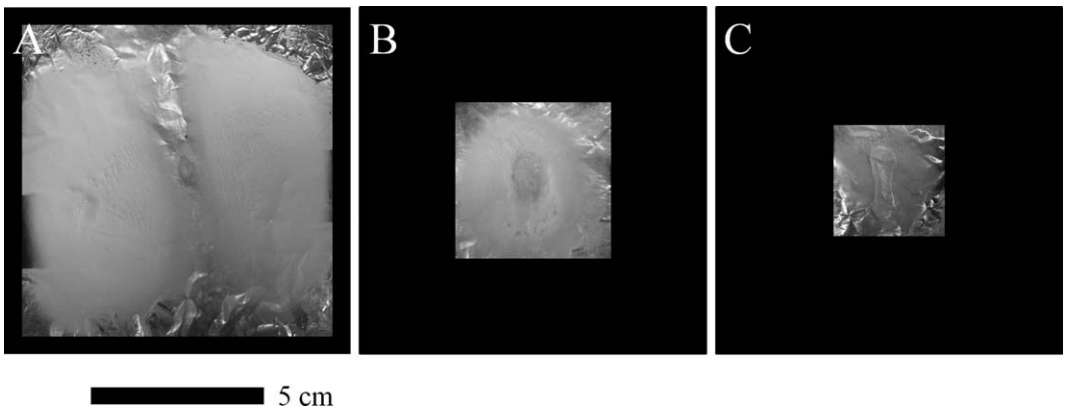

Figure 9. Images show the reduction of the surface area of electrospun web formed from PEO nanofibers containing 20% urea as the electric field strength between the charged target and grounded needle is increased from (A) 1 kV/cm to (B) 1.31 kV/cm, and, finally, to (C) 1.64 kV/cm.

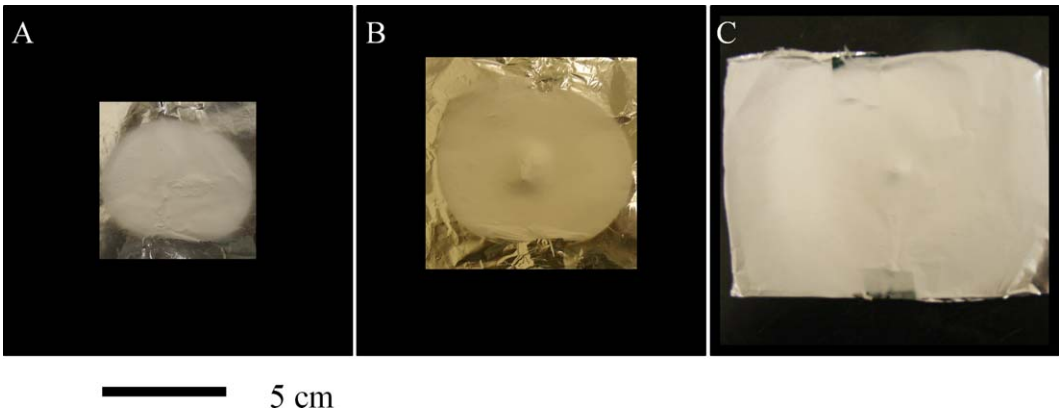

Figure 10. Images show the increase of the web area of PEO nanofibers containing 20 wt % urea with the increase of the electric field strength between the grounded target and charged needle as the electric field strength is increased from (A) 1 kV/cm, (B) 1.31 kV/cm, to (C) 1.64 kV/cm. [Color figure can be viewed in the online issue, which is available at wileyonlinelibrary.com.]

diameters are in the range of 200–400 nm; however, the fibers' morphology was deformed into thick bundles. This could be attributed to existence of certain amount of water bounded to urea and confined inside nanofibers. The formation of three dimension network can be explained as follows: by increase the amount of urea, then the solution conductivity will be increased.[39–41] Because of the strong repulsion between charges during electrospinning, the length of the electric field induced instability region will be reduced which is resulting in the increase of the electrospinning process speed.[42] As a result of fast electrospinning the fibers will be deposited randomly in 3D structure on the target.

Impact of Polarities Reverse and Electric Field Strengths

The effect of the polarity of the electrodes is studied for the electrospun fibers of PEO containing 20 wt % of urea. In the first configuration, the target is charged while the needle is grounded. Conversely, the needle is charged and the target is grounded in the second configuration. For each polarity configuration, the PEO solution is electrospun at three different electric field strengths (1, 1.31, and 1.64 kV/cm). All samples are electrospun for the same processing time of 30 min.

In the first configuration, it is observed that the surface area of the webs produced is reduced as the electric field strength increases, as shown in Figure 9. This can be explained as the dominant force is one of attraction between the charges in the PEO jet and the higher potential surface of the target. This can lead to a shift in all instability zones (the electric field-induced, varicose, and whipping instabilities) to a location closer to the target. As a result of this shift, the base area of the inverted envelope in the whipping instability is reduced. Consequently, the area of deposition is reduced. The existence of two separate lobes in the web seen in Figure 9(A) is due to branching of the polymer jet in the bending instability zone.

Changing the polarity of the electric field to the second configuration produces a larger area of the deposited web with increasing electric field strength (Figure 10). Because of the increase of the charge concentration at the droplet tip, there is a larger concentration of charges that accumulate on the surface of the polymer jet. Thus, the repulsion force becomes dominant in this configuration, resulting in the development of larger bending instability zone. As a result, the base area of the inverted envelope cone is increased. The regions of the electric field-induced instability and the varicose instability are not changed significantly. It can be observed that a mound is formed at higher electric field strength, as seen in the center of Figure 10(B,C).

CONCLUSIONS

The electrospinning behavior of PVA and PEO nanofibers embedded with urea has been studied as a function of urea concentration, electrodes polarity, and electric fields. Analysis of the FTIR spectra collected on the nanofibers proves the existence of hydrogen bonding between urea and polymer matrix, which are broken at elevated temperatures. The bonds between PEO and urea are less thermally stable than the bonds between PVA and urea. A three-dimensional network is formed when electrospinning with solutions containing PEO with weight ratio of urea up to 25 wt %, where the networking increases with increasing urea concentration. Negligible networking is observed in the PVA solutions with urea, although there is considerable fusing of the PVA nanofibers at high concentrations of urea. Also, this work shows that the area of deposition and three-dimensionality of the electrospun webs embedded with urea can be controlled by manipulating the polarity and magnitude of the electric field between the electrodes, the needle and the target. The results demonstrate that polymer nanofibers can be electrospun from solutions of PEO and PVA that contain high concentration of urea, which may have an application as means to safely distribute urea fertilizer in nanoagriculture. From FTIR results, PEO is concluded is better than PVA as a biodegradable polymer to embed high concentrations of active urea when forming electrospun mats that will release the urea for use as fertilizer.

ACKNOWLEDGMENTS

The authors acknowledge the Department of Chemistry in Virginia Tech (VT) for the ATR-FTIR measurements, the Virginia Tech Institute for Critical Technology and Applied Science

(ICTAS), Nanoscale Characterization and Fabrication Laboratory (NCFL) for FESEM characterization. Also, the authors are grateful to the financial support from ICTAS, Bradley Department of Electrical and Computer Engineering at Virginia Tech and the Virginia Tech Middle East and North Africa (VT-MENA) program in Egypt.

REFERENCES

1. Weiss, J.; Bruulsema, T.; Hunter, M.; Czymmek, K.; Lawrence, J.; Ketterings, Q. Agronomy Fact Sheet Series, Cornell University Cooperation Extension **2009**, 1.
2. James, D. W. Fertilizer Fact Sheet, Utah State University **2010**, 1.
3. Castro-Enríquez, D.; Rodríguez-Félix, F.; Ramírez-Wong, B.; Torres-Chávez, P.; Castillo-Ortega, M.; Rodríguez-Félix, D.; Armenta-Villegas, L.; Ledesma-Osuna, A. *Materials* **2012**, *5*, 2903.
4. Cowden, J.; Hotchkiss, A. K.; Keshava, C.; Lee, J. S.; Marcus, A.; Rooney, A.; Sams, R. U.S.E.P. *Agency* **2011**, 1.
5. Sangeetha, S.; Sujatha, K.; Senthilkumaar, P.; Kalyanaraman, V.; Eswari, S. *Indian J. Sci. Technol. Vol.* **2011**, *4*, 770.
6. Suherman, I.; Anggoro, D. D. *Int. J. Eng. Technol.* **2011**, 77.
7. Larrondo, L.; St. John Manley, R. *J. Polym. Sci. Polym. Phys. Ed.* **1981**, *19*, 909.
8. Shin, Y. M.; Hohman, M. M.; Brenner, M. P.; Rutledge, G. C. *Appl. Phys. Lett.* **2001**, *78*, 1.
9. Liu, W.; Graham, M.; Evans, E. A.; Reneker, D. H. *J. Mater. Res.* **2002**, *17*, 3206.
10. Frenot, A.; Chronakis, I. S. *Current Opin. Colloid Interface Sci.* **2003**, *8*, 64.
11. Hohman, M. M.; Shin, M.; Rutledge, G.; Brenner, M. P. *Physics Fluids* **2001**, *13*, 2201.
12. Huang, Z.-M.; Zhang, Y.-Z.; Kotaki, M.; Ramakrishna, S. *Compos. Sci. Technol.* **2003**, *63*, 2223.
13. Lyons, J. M. Melt-Electrospinning of Themoplastic Polymers: An Experimental and Theoretical Analysis. PhD. Thesis, Department of Materials Science and Engineering, Drexel University **2004**, 1–211.
14. Li, D.; Ouyang, G.; McCann, J. T.; Xia, Y. *Nano Lett.* **2005**, *5*, 913.
15. Teo, W. E.; Ramakrishna, S. *Nanotechnology* **2006**, *17*, 89.
16. Kowalewski, T. A.; Blonski, S.; Barral, S. *Bull. Polish Acad. Sci.* **2005**, *53*, 385.
17. Feil, K. Melt Electrospinning of Scaffolds for Tissue Engineering. Diploma Thesis, Faculty of Mathmatic, Informatic and Natural Sciences, RWTH-Aachen **2005**, 1–88.
18. Ramakrishna, S.; Fujihara, K.; Teo, W.-E.; Lim, T.-C.; Ma, Z. An Introduction to Electrospinning and Nanofibers; World Scientific Publishing Co. Pte. Ltd: Ton Tuck Link, Singapore, **2005**; p 1.
19. Lyons, J.; Ko, F. *Polym. News* **2005**, *30*, 1.
20. Chronakis, I. S. *J. Mater. Proc. Technol.* **2005**, *167*, 283.
21. Liu, Y.; Antaya, H.; Pellerin, C. *J. Polym. Sci. Part B: Polym. Phys.* **2008**, *46*, 1903.
22. Isakov, D.; de Matos Gomes, E.; Belsley, M.; Almeida, B.; Martins, A.; Neves, N.; Reis, R. *EPL (Europhysics Lett.)* **2010**, *91*, 1.
23. Celebioglu, A.; Uyar, T. *Langmuir* **2011**, *27*, 6218.
24. Watanabe, S.; Yamazaki, M.; Kaihara, S.; Fujimoto, K. *Colloids Surfaces A: Physicochem. Eng. Aspects* **2012**, *399*, 83.
25. Matsumura, S.; Shimura, Y.; Terayama, K.; Kiyohara, T. *Biotechnol. Lett.* **1994**, *16*, 1205.
26. Mori, T.; Sakimoto, M.; Kagi, T.; Sakai, T. *Biosci. Biotechnol. Biochem.* **1996**, *60*, 330.
27. Nakamiya, K.; Toshihiko, O.; Kinoshita, S. *J. Fermentation Bioeng.* **1997**, *84*, 213.
28. Marchal, R.; Nicolau, E.; Ballaguet, J.-P.; Bertoncini, F. *Int. Biodeterioration Biodegradation* **2008**, *62*, 384.
29. Zgoła-Grześkowiak, A.; Grześkowiak, T.; Zembrzuska, J.; Łukaszewski, Z. *Chemosphere* **2006**, *64*, 803.
30. Tao, J. Effects of Molecular Weight and Solution Concentration on Electrospinning of PVA. Master Thesis, Material Science and Engineering, Worcester Polytechnic Institute **2003**, 1–107.
31. Matsumura, S.; Kurita, H.; Shimokobe, H. *Biotechnol. Lett.* **1993**, *15*, 749.
32. Lum, L.; Elisseeff, J. Injectable Hydrogels for Cartilage Tissue Engineering. I Cartilage, Topics in Tissue Engineering 2003. Eds. N. Ashammakhi & P. Ferretti, Chapter *4*, **2003**, p 1.
33. Gibas, I.; Janik, H. *Chem. Chem. Technol.* **2010**, *4*, 297.
34. Slaughter, B. V; Khurshid, S. S.; Fisher, O. Z.; Khademhosseini, A.; Peppas, N. *Adv. Mater.* **2009**, *21*, 3307.
35. Martens, P. J.; Bryant, S. J.; Anseth, K. S. *Biomacromolecules* **2003**, *4*, 283.
36. Carey, F. A. *Organic Chemistry*; Peterson, K. A., Ed.; 4th ed.; James M. Smith, **2000**; p 619.
37. Tudorachi, N.; Cascaval, C.; Rusu, M.; Pruteanu, M. *Polym. Test.* **2000**, *19*, 785.
38. Merrett, K.; Cornelius, R. M.; Mcclung, W. G.; Unsworth, L. D.; Sheardown, H. *J. Biomater. Sci. Polym. Ed.* **2002**, *13*, 593.
39. Venkatesan, V. K.; Suryanarayana, C. V. *J. Phys. Chem.* **1956**, *60*, 775.
40. Thavarungkul, P.; Kanatharana, P. *J. Sci. Soc. Thailand* **1994**, *20*, 23.
41. Chin, W.-T.; Kroontje, W. *Anal. Chem.* **1961**, *33*, 1757.
42. Lee, H.; Kim, G. J. *Biomater. Sci. Polym. Ed.* **2010**, *21*, 1687.